Published in final edited form as:
Nat Immunol. 2013 December ; 14(12): 1237–1246. doi:10.1038/ni.2756.

ELF4 is critical for induction of type I interferon and the host antiviral response

Fuping You[1], **Penghua Wang**[1], **Long Yang**[1], **Guang Yang**[1,6], **Yang O Zhao**[1,2], **Feng Qian**[3], **Wendy Walker**[1,2], **Richard Sutton**[1], **Ruth Montgomery**[3], **Rongtuan Lin**[4], **Akiko Iwasaki**[2,5], and **Erol Fikrig**[1,2]

[1]Section of Infectious Diseases, Yale University School of Medicine, New Haven, Connecticut, USA. [2]Howard Hughes Medical Institute, Chevy Chase, Maryland, USA. [3]Section of Rheumatology, Department of Internal Medicine, Yale University School of Medicine, New Haven, Connecticut, USA. [4]Lady Davis Institute, Department of Medicine, McGill University, Montreal, Quebec, Canada. [5]Department of Immunobiology, Yale University School of Medicine, New Haven, Connecticut, USA.

Abstract

Induction of type I interferon is a central event of innate immunity, essential for host defense. Here we report that the transcription factor ELF4 is induced by type I interferon and upregulates interferon expression in a feed-forward loop. ELF4 deficiency leads to reduced interferon production, resulting in enhanced susceptibility to West Nile virus encephalitis in mice. After viral infection, ELF4 is recruited by STING, interacts with and is activated by the MAVS-TBK1 complex, and translocates into the nucleus to bind interferon promoters. Cooperative binding with ELF4 increases the binding affinity of interferon regulatory factors IRF3 and IRF7, which is mediated by EICE elements. Thus, in addition to identifying a regulator of innate immune signaling, we uncovered a role for EICE elements in interferon transactivation.

The innate immune system serves as the first-line sentinel of host defense against invading pathogens by recognizing various conserved molecular motifs called pathogen-associated molecular patterns (PAMPs) and initiating cellular host defense countermeasures. PAMPs are detected by several classes of host pattern recognition receptors (PRRs), including Toll-like receptors (TLRs), RIG-like receptors (RLRs), NOD-like receptors (NLRs), C-type lectins and double-stranded DNA (dsDNA) receptors. The PRR responses trigger the activation of downstream signaling events, leading to the transcription of NF-κB–dependent and IRF3-IRF7–dependent genes, including type I interferon[1].

Correspondence should be addressed to E.F. (erol.fikrig@yale.edu)..
[6]Present address: Department of Parasitology, School of Medicine, Jinan University, Guangzhou, China.

AUTHOR CONTRIBUTIONS

F.Y. and E.F. designed the study, analyzed the data and wrote or revised the paper. F.Y. performed most experiments. R.L., L.Y. and P.W. analyzed the data. P.W. provided technical support and contributed to animal work. P.W. and L.Y. contributed equally to the second authorship. F.Q. G.Y. and Y.O.Z. provided expertise and contributed to flow cytometry and immunofluorescence experiments and viral infections. L.Y. and W.W. provided technical help. R.M., R.S. and A.I. provided expertise and contributed to experiment with viral infection.

Note: Any Supplementary Information and Source Data files are available in the online version of the paper.

COMPETING FINANCIAL INTERESTS

The authors declare no competing financial interests.

TLRs recognize a range of products derived from a variety of pathogens, including bacteria, fungi, viruses and parasites[2]. All TLRs characterized so far signal through the adaptor proteins MyD88 or TRIF, the latter downstream of TLR3 and TLR4. RLRs recognize cytoplasmic viral RNA and recruit the adaptor MAVS (also called Cardif, IPS-1 or VISA)[3–6]. Currently known dsDNA receptors include AIM2, which forms an inflammasome with ASC and caspase-1 (ref. 7), RNA polymerase III, which converts DNA into 5′-triphosphorylated RNA that activates RIG-I (ref. 8) and the DNA cytoplasmic sensors IFT16 (ref. 9), DDX41 and cGAS[10,11]. Signals from IFI16, DDX41 and cGAS are transduced by the endoplasmic reticulum membrane protein STING (also termed ERIS, MITA, MPYS or TMEM173), which has a key role in the cytoplasmic nucleic acid sensing pathway[12–15]. Most innate immune signaling pathways result in the induction of type I interferon and other cytokines. Type I interferon is induced within hours after infection, often in high amounts, to initiate an antiviral state in cells and is essential for survival in acute viral infection and modulation of the immune response.

IRF3 and IRF7 are critical transcriptional factors that regulate production of type I interferon (IFN-α and IFN-β) by binding to the inter-feron stimulated response element (ISRE). *Irf3*$^{-/-}$, *Irf7*$^{-/-}$ or *Irf3*$^{-/-}$ × *Irf7*$^{-/-}$ mice are much more prone to viral infection than wild-type mice, and do not induce type I interferon efficiently. However, *Irf3*$^{-/-}$ × *Irf7*$^{-/-}$ macrophages and dendritic cells have minimally diminished induction of IFN-β after viral infection, indicating that other transcription factors may be necessary for interferon expression[16]. ELF4 (refs. 17,18) belongs to the ETS transcription factor family, which has at least 27 mammalian members involved in various biological processes[19]. ELF4 controls the quiescence of endothelial cells[20], promotes cellular transformation[18] and is associated with ovarian cancer and leukemias[21,22]. These studies suggest that ELF4 is an important transcription factor, though its physiological functions are largely unknown. A previous study has shown that the ETS transcription factor PU.1 cooperates with IRF4 to regulate the expression of immunoglobulin[23], suggesting a correlation between the ETS binding motif and the ISRE.

Here we demonstrate that ELF4 regulates interferon induction and is critical for host defense. ELF4 was activated in response to innate immune signals and initiated transcription of type I inter-feron genes to control diverse pathogens. *Elf4*$^{-/-}$ mice had increased susceptibility to viral infection. In the absence of ELF4, IRF3, IRF7 and NF-κB bind inefficiently to interferon gene promoters, resulting in impaired type I interferon responses. ELF4 has a global role in TLR, RLR and STING-mediated DNA sensing signaling pathways, indicating its fundamental importance in the innate immune system.

RESULTS

ELF4 binds to STING and induces interferon

We investigated the role of STING, an adaptor protein that has a pivotal role in antiviral immune signaling, in infection with West Nile virus (WNV), a single-stranded RNA virus that can cause lethal meningoencephalitis in humans. STING loss-of-function *Tmem173*$^{gt/gt}$ mice (also known as *Goldenticket* and here referred to as *Sting*$^{gt/gt}$)[24] were more susceptible to WNV than wild-type animals (**Fig. 1a**). To more clearly understand STING-related antiviral immunity and to identify interacting factors of this antiviral pathway, we used an infection interaction screen to detect virus-induced genes that associate with STING. We infected HeLa cells that expressed Flag epitope–tagged STING with WNV, and purified Flag-STING by immunoprecipitation. Analysis of STING-associated proteins resolved by SDS-PAGE and analyzed by mass spectrometry identified ELF4 as a protein recruited to STING after infection with WNV (**Fig. 1b** and **Supplementary Tables 1** and **2**). We

confirmed the interaction between ELF4 and STING by co-immunoprecipitation in HeLa cells (**Fig. 1c**).

293T cells transfected with plasmids encoding either human or mouse ELF4 activated a luciferase reporter driven by the *Ifnb1* promoter (IFN-β–Luc), which resulted in up to 200-fold induction of the reporter, comparable to levels induced by overexpressed MAVS (**Fig. 1d** and **Supplementary Fig. 1b**)[25]. Real-time PCR analysis showed that ELF4 induced *Ifnb1* mRNA in 293T cells (**Fig. 1e** and **Supplementary Fig. 1a**). The ELF4-mediated activation of *Ifnb1* was specific, as related ELF family members that also have ETS DNA-binding domains did not induce *Ifnb1* (**Fig. 1f**). To assess whether ELF4 led to the production and secretion of interferon proteins, we measured amounts of type I interferon in the supernatants after overexpression of ELF4 via a bio-assay using 2fTGH cells with a luciferase reporter driven by the ISRE (2fTGH-ISRE-Luc cells), which generate luciferase in response to type I interferons. The release of type I interferon was markedly increased after ELF4 overexpression (**Fig. 1g**). To study the function of ELF4 in immune responses, we examined induction of cytokines related to interferon, including various forms of IFN-α and IFN-λ3. Exogenous expression of ELF4 modestly upregulated INF-α2, IFN-α8 and IFN-λ3, and did not upregulate IFN-α4 or IL-22 (**Supplementary Fig. 1d–h**).

To determine the breadth of the antiviral signals transduced by ELF4, we quantified secretion of interferon in ELF4-expressing cells triggered by the following: an RNA virus, a DNA virus, HIV, poly(I:C) or poly(dA:dT) (**Fig. 1h** and **Supplementary Fig. 1c**). ELF4 enhanced induction of interferon triggered by all viral stimuli and agonists tested. To identify the critical domains of ELF4 required for the induction of type I interferon, we determined the ability of several ELF4 variants (**Supplementary Fig. 2a**) to induce type I interferon. The ETS domain, which mediates binding between ELF4 and *cis*-acting elements, was essential for production of IFN-β induced by ELF4, as assessed by reporter assay. In addition, we observed marked abrogation of IFN-β induction when we deleted the nuclear localization sequence region (NLS, as delineated on the Eukaryotic Linear Motif resource website; http://elm.eu.org/), TRAF2 binding motif (T2B; http://elm.eu.org/) or amino acids 1–87 (amino acids 1–52 comprise a putative transactivation domain)[26]. Proteins lacking the C terminus of ELF4, which is responsible for the interaction with STING (**Supplementary Fig. 2b**), induced the IFN-β reporter poorly, but both the putative transmembrane helices and the sumoylation sites were dispensable (**Fig. 1i**). Collectively, these results demonstrate that ELF4 is a potent stimulator of type I interferon.

ELF4 is involved in antiviral immune signaling

As ELF4 stimulates production of interferon, which is critical for anti-viral immunity, we examined the response of ELF4 to viral infection. *Elf4* mRNA was highly induced when we infected cells with either Sendai virus (SeV) or vesicular stomatitis virus (VSV) (**Fig. 2a**), suggesting the involvement of this protein in antiviral responses. Primary monocyte–derived macrophages from human donors showed significant induction of *Elf4* and *Ifnb1* mRNA after infection with WNV (**Fig. 2b**). We also observed that expression of ELF4 was induced by interferon, indicating that *Elf4* is an interferon-stimulated gene (**Fig. 2c**). In addition, the replication of SeV, VSV and WNV was dramatically attenuated by ELF4 overexpression. Inhibition of viral replication was dose-dependent as measured by immunoblot and a plaque assay (**Supplementary Fig. 3a–c**).

To further delineate the function of ELF4 in host defense, we infected KEK 293T cells after knockdown of endogenous *Elf4* by small interfering (si)RNA. Transfection of an ELF4-specific siRNA reduced ELF4 expression and resulted in increased viral replication, when compared to transfection with control (scrambled) siRNA (**Fig. 2d** and **Supplementary Fig.**

3d,e). Consistent with this, VSV and HSV-1 replication were markedly enhanced in *Elf4*$^{-/-}$ mouse embryonic fibroblasts (MEFs) and mouse macrophages compared with wild-type cells (**Fig. 2e–h** and **Supplementary Fig. 3f–h**). *Elf4*$^{-/-}$ MEFs reconstituted with full-length ELF4, but not the variant with the ETS domain deleted, reduced VSV or HSV-1 infectivity significantly (**Fig. 2e–g**), indicating that the ETS domain is essential for the antiviral activity of ELF4. IFN-β production induced by viral infection was impaired in *Elf4*$^{-/-}$ MEFs, and could be restored by full-length ELF4 but not the variant with ETS deleted (**Fig. 2i**). ELF4 therefore has a role in host defense against viral infection.

ELF4 is critical for antiviral immunity *in vivo*

To evaluate the importance of ELF4 in viral infection *in vivo*, we infected wild-type and *Elf4*$^{-/-}$ mice with WNV. In keeping with our *in vitro* data, and consistent with the results using *Sting*$^{gt/gt}$ and Mavs$^{-/-}$ mice[27], *Elf4*$^{-/-}$ mice were significantly more susceptible to lethal WNV infection compared to wild-type mice (**Fig. 3a**). Viremia was significantly higher in *Elf4*$^{-/-}$ mice than in wild-type mice at day 3 after infection, as determined by real-time PCR of transcripts encoding WNV envelope proteins (here referred to as WNVE transcripts; **Fig. 3b**). Because meningoencephalitis contributes to WNV lethality[28], we quantified viral burdens in brains of wild-type and *Elf4*$^{-/-}$ mice. Consistent with the survival data, the viral burden (as assessed by WNVE mRNA and plaque assays) was higher in the central nervous system of *Elf4*$^{-/-}$ mice than wild-type mice at day 8 after infection (**Fig. 3c,d**). We observed similar differences in the spinal cord, kidney and splenic tissues (**Fig. 3e–g**). Consistently, we observed more immune cell infiltrate in the central nervous system (**Fig. 3h,i**) and a more pronounced antiviral serologic response (**Supplementary Fig. 3i,j**) in the *Elf4*$^{-/-}$ mice. In addition, we detected less circulating IFN-β and IFN-α2 in the blood or plasma of *Elf4*$^{-/-}$ mice on days 1 and 3 after WNV infection (**Fig. 3j–l**) and less interferon-induced protein ISG15 (**Fig. 3m**). Induction of *Ifng*, *Il6* and the IFN-γ–inducible gene *Cxcl10*, however, was similar in *Elf4*$^{-/-}$ and wild-type mice (**Fig. 3n** and **Supplementary Fig. 3k,l**). Consistent with the *in vitro* data, the *Elf4* mRNA in blood was upregulated at day 1 and 3 after WNV infection compared to day 0 (**Fig. 3o**). Furthermore, induction of type I interferon and antiviral activity were impaired in macrophages isolated from *Elf4*$^{-/-}$ mice after WNV infection (**Fig. 3p,q**). Thus, ELF4 is involved in the induction of type I interferon and protection against infection with WNV.

ELF4 has been shown to regulate two important antiviral mechanisms: development of NK and NK T cells[29], and proliferation and homing of CD8$^+$ T cells by activating Klf4 expression[17]. NK and NKT cell numbers are profoundly reduced in *Elf4*$^{-/-}$ mice compared to wild-type mice[29]. However, NK and NKT cells appear to be dispensable for the host anti-WNV immune response[30] likely because WNV and other flaviviruses partially suppress NK cell activity in mice[31]. Consistently, reconstitution of NK and NKT cells in *Elf4*$^{-/-}$ mice by tail-vein injection did not affect the susceptibility of these mice to WNV (**Supplementary Fig. 3m**). In addition, *Elf4*$^{-/-}$ mice had a similar number of NK cells as wild-type mice after WNV infection (**Fig. 3r**). CD8$^+$ T cells in particular are required for WNV clearance from the central nervous system[32]. However, differences in proliferation of CD8$^+$ T cells between *Elf4*$^{-/-}$ and wild-type mice are only notable in mice older than 6 months[17]. Consistent with this, we observed a similar proportion of splenic CD8$^+$ T cells in *Elf4*$^{-/-}$ and wild-type mice before and after viral infection as well as comparable proportions of CD4$^+$ T cells (**Supplementary Fig. 3n,o**). *Elf4*$^{-/-}$ and wild-type mice in our experiments were 6 weeks old and had similar extent of CD8$^+$ T cell proliferation[17]. These data suggest that ELF4 controls WNV replication primarily via regulation of type I inter-feron response and not through modulation of NK cell, NKT cell or CD8$^+$ T cell numbers during viral infection. Nevertheless, ELF4 may participate in the regulation of CD8$^+$ T cell function indirectly via

induction of type I interferons[33] and also by influencing NK and NKT cell survival and proliferation via type I interferon–induced IL-15 (ref. 34).

ELF4 is involved in TLR, RLR and dsDNA receptor signaling

To study the functions of ELF4, we next evaluated the role of ELF4 in innate immune signaling pathways, such as TLR-, RLR- and STING-dependent dsDNA-sensing pathway. Activation of the *Ifnb1* promoter by poly(I:C), SeV, poly(dA:dT) or HSV-1 was attenuated when we silenced *Elf4* by a specific siRNA (**Fig. 4a** and **Supplementary Fig. 4a**), indicating that ELF4 was required for RLR- and STING-dependent activation of *Ifnb1* transcription. Bone marrow–derived macrophages (BMDMs) from *Elf4*$^{-/-}$ animals showed significantly impaired production of IFN-β compared to wild-type BMDMs when triggered by poly(I:C), lipopolysaccharide (LPS) or CpG DNA as well as after infection with SeV, EMCV or HSV-1 compared to wild-type BMDMs (**Fig. 4b**). Therefore, ELF4 is also required for IFN-β production mediated by TLR3, TLR4, TLR7 and TLR9. We observed similar results when we measured the activation of IFN-β, IFN-α2 and ISG15 by TLR or RLR agonists in BMDMs, peritoneal macrophages and bone marrow–derived dendritic cells (BMDCs), indicating a global role of ELF4 in innate antiviral response (**Fig. 4c–f**). Consistent with this, production of IFN-β induced by LPS, R848 or poly(I:C) decreased markedly after siRNA-mediated knockdown of ELF4 in 293T cells that stably express TLR4, TLR7 or TLR3 (**Fig. 4g**). However, ELF4 was dispensable for induction of IL-1β and tumor necrosis factor (TNF) in macrophages, suggesting a specific role in type I interferon–related gene regulation (**Fig. 4h** and **Supplementary Fig. 4b**). In contrast to the *in vivo* results, induction of *Cxcl10* was impaired in *Elf4*$^{-/-}$ MEFs (**Supplementary Fig. 4c**). As *Cxcl10* is induced in response to IFN-α signaling and also IFN-γ signaling, the deficiency of *Cxcl10* induction resulting from impaired IFN-α may be compensated by IFN-γ in *Elf4*$^{-/-}$ mice.

To characterize the role of ELF4 in signaling pathways downstream of pathogen-recognition receptors, we quantified the induction of an IFN-β reporter in a luciferase assay in untransfected or in ELF4 plasmid–transfected MEFs derived from animals deficient in the innate adaptors MyD88, TRIF, MAVS or STING. ELF4-induced activation of IFN-β was similar in the adaptor-deficient cells and in wild-type cells (**Fig. 4i**). We obtained similar results when we subjected 293T cells to siRNA-mediated knockdown of TRIF, MAVS, MyD88 or STING (**Supplementary Fig. 4d**), which indicated that ELF4 functions downstream of these adaptors. In ELF4-deficient MEF cells transfected with plasmids encoding the adaptors TRIF, MAVS, MyD88 or STING and luciferase reporters for IFN-β or ISRE, activity induced by adaptor overexpression was decreased compared to wild-type cells (**Fig. 4j**). Consistent with this, siRNA-mediated knockdown of ELF4 in 293T cells reduced the production of IFN-β induced by TRIF, MAVS or STING overexpression, as well as the activation of ISRE induced by MyD88 (**Supplementary Fig. 4e–h**). Thus, ELF4 appears to function downstream of TRIF, MyD88, MAVS and STING.

ELF4 is activated by virus infection and parallel with IRFs

Because ELF4 associates with STING in virus-infected cells, we investigated the possibility that ELF4 regulated the activation of NF-κB or IRF3. As a positive control, ectopic expression of MAVS activated IRF3 and NF-κB in a dose dependent manner (**Fig. 5a**) as revealed by the phosphorylation of IRF3 and NF-κB. However, ectopic expression of ELF4 did not activate IRF3 and NF-κB (**Fig. 5a**). Furthermore, SeV-induced IRF3 dimerization was blocked in MAVS-deficient MEFs or in 293T cells in which *Mavs* was knocked down but not in ELF4-deficient MEFs or in 293T cells in which *Elf4* was knocked down (**Fig. 5b** and **Supplementary Fig. 5a**). These results indicate that ELF4 is not involved in the activation of IRF3 and NF-κB. We next examined the possibility that association with

STING may recruit ELF4 to the MAVS-TBK1 signaling complex and activate ELF4. ELF4 coimmunoprecipitated with MAVS or TBK1 in the presence of STING (**Supplementary Fig. 5b**). Further, viral infection promoted ELF4 interaction with STING as well as with TBK1 (**Fig. 5c**). Overexpression of ELF4 did not induce type I interferon in *Tbk1*$^{-/-}$ MEFs (**Fig. 5d**). Reconstitution of *Tbk1*$^{-/-}$ MEFs with wild-type TBK1, but not with a TBK1 variant lacking kinase activity, restored the ability of ELF4 to induce IFN-β (**Fig. 5d**). ELF4 is phosphorylated after viral infection (**Supplementary Fig. 5c**), which prompted us to examine whether TBK1 could phosphorylate ELF4. *In vitro* kinase assays showed that TBK1 mediated phosphorylation of ELF4 (**Fig. 5e**). We examined four main phosphorylation regions in ELF4 (using the NetPhos 2.0 Sever) to identify amino acids phosphorylated by TBK1. The third ELF4 phosphorylation region is necessary for induction of IFN-β expression (**Supplementary Fig. 5d**), in which Ser331 is indispensable (**Fig. 5f** and **Supplementary Fig. 5e**). To confirm that TBK1 is needed for activation of ELF4, we examined type I interferon induction in plasmacytoid dendritic cells (pDCs), which are known to not use TBK1 for regulation of interferons[35]. CpG DNA–induced production of interferons was normal in *Elf4*$^{-/-}$ pDCs (**Supplementary Fig. 5f,g**) indicating that TBK1 and ELF4 are not involved in signaling of type I interferon in this cell type.

In addition, the dimerization of endogenous ELF4 was induced by viral infection as well as by stimulation with poly(I:C), LPS, R848 and CpG DNA in macrophages (**Fig. 5g**). The ETS domain was required for ELF4 dimerization (**Supplementary Fig. 5h,i**). We observed nuclear translocation of ELF4 after SeV infection and ELF4 overexpression in HeLa cells (**Fig. 5h** and **Supplementary Fig. 5j**). Furthermore, MAVS, STING, TBK1 and phosphorylation of ELF4 were essential for the nuclear translocation of ELF4 in response to viral infection, as assessed by western blotting and immunofluorescence (**Fig. 5i** and **Supplementary Fig. 5k,l**). In contrast with endogenous ELF4, ectopically expressed ELF4 resided in the nucleus (**Fig. 5j**). ELF4 contains two putative nuclear-localization sequences (NLSs): at amino acids 196–202 (NLS1)[26] and 173–183 (NLS2; http://elm.eu.org/). We examined subcellular localization of ELF4 variants with deleted NLS1 (ELF4-ΔNLS1), NLS2 (ELF4-ΔNLS2) or both NLS1 and NLS2 (ELF4-ΔNLS1-2). ELF4-ΔNLS1-2 and ELF4-ΔNLS2 were retained in the cytoplasm, whereas ELF4-ΔNLS1 localized both in the nucleus and cytoplasm (**Fig. 5j**). ELF4-ΔNLS1-2 and ELF4-ΔNLS2 did not activate the Ifnb1 promoter, whereas ELF4-ΔNLS1 induced weak promoter activity (**Supplementary Fig. 5m**). Taken together, these results suggest that in response to viral infection, ELF4 was phosphorylated by TBK1 and translocated to the nucleus in a MAVS- and STING-dependent manner.

ELF4 binds to type I interferon promoters

The ETS domain mediates sequence-specific DNA binding[36] with two highly conserved arginines in this domain critical for DNA binding[34]. Overexpression of an ELF4 variant in which both of these conserved arginines were replaced by alanines (ELF4-RRAA) in 293T cells abrogated activation of IFN-β. Induction of IFN-β was restored when we replaced the alanine with arginine in the mutants (**Fig. 6a**), suggesting that ELF4-dependent induction of interferon depends on DNA binding by ELF4. Chromatin immunoprecipitation and quantitative PCR (ChIP-qPCR) indicated that ELF4 and IRF3 were recruited to the *Ifnb1* and *Ifna2* promoters (**Fig. 6b,c**) in macrophages infected with SeV. Electrophoretic mobility shift assays (EMSAs) also showed that ELF4 bound to the *Ifnb1* promoter after infection with SeV (**Fig. 6d,e**).

ETS transcription factors bind to related, but distinct, sites containing a core purine-rich motif, GGAA. We identified three GGAA motifs in the *Ifnb1* promoter, four GGAA motifs in the *Ifna2* promoter and one GGAA motif in the *Ifna4* promoter (**Supplementary Fig. 5n**).

Activation of the *Ifnb1* promoter was impaired when the first (position −80 relative to the transcription start site) or second (position −50) GGAA was replaced by GATC (**Fig. 6f**). In EMSA, *in vitro*–expressed ELF4 protein bound to the wild-type *Ifnb1* promoter probe, did not bind a probe that contained mutations in the first GGAA motif (IFN-mut1) and bound weakly to probes that contained mutations in the second (IFN-mut2) or third (IFN-mut3) GGAA motifs (**Fig. 6g**). These data suggest that ELF4 binds to the *Ifnb1* promoter directly. Furthermore, activation of *Ifna2* was significantly reduced after replacing the second GGAA with GATC (**Fig. 6h**), indicating that ELF4 also binds the *Ifna2* promoter. Taken together, our results demonstrate that ELF4 binds and activates interferon gene promoters.

ELF4 synergizes with IRFs and NF-κB to induce interferon

Combinatorial interactions between distinct classes of sequence-specific transcription factors are important in regulating eukaryotic gene expression in response to diverse environmental signals[37]. The *Ifnb1* promoter contains DNA-binding sites for several transcription factors: NF-κB, IRF3-IRF7 and activator protein 1 (AP1; a heterodimeric protein composed of ATF-2 and c-Jun)[38] (**Supplementary Fig. 5n**). We observed that ELF4 could activate a luciferase reporter of the interferon regulatory factor (IRF)-binding element (ISRE-Luc) and NF-κB–Luc but not AP1-Luc (**Supplementary Fig. 6a**). We first examined the role of IRF3 and p65 on ELF4-mediated activation of *Ifnb1* promoter in 293T cells, which do not express IRF7. Knockout of *Irf3* in MEFs or knockdown of *Rela* in 293T cells reduced the ability of ELF4 to activate the *Ifnb1* promoter (**Fig. 7a,b** and **Supplementary Fig. 6b**). Overexpression of ELF4 strongly synergized with IRF3 to activate the *Ifnb1* promoter in 293T cells (**Supplementary Fig. 6c**). Flag-tagged ELF4 co-immunoprecipitated with hemagglutinin (HA)-tagged p65 but did not associate with HA-tagged p50 or IRF3 in 293T cells (**Supplementary Fig. 6d**). Endogenous ELF4 associated with p65 after infection with SeV in 2fTGH cells (**Fig. 7c**). SeV-mediated recruitment of ELF4 to the *Ifnb1* promoter, but not to the *Ifna2* or *Ifna4* promoters, was attenuated by siRNA-mediated silencing of p65 in MEFs (**Fig. 7d** and **Supplementary Fig. 6e**). Conversely, p65 did not bind efficiently to the *Ifnb1* promoter in *Elf4*$^{-/-}$ MEFs (**Fig. 7e**). However, ELF4 had no effect on p65-mediated activation of NF-κB–Luc reporter activity (**Supplementary Fig. 6f**), indicating that both NF-κB binding and ELF4 binding are required for the cooperative activation of interferon promoters.

The ETS domain protein PU.1 can recruit IRF family transcription factors IRF2, IRF4 and IRF8 to specific promoters carrying composite ETS-IRF elements (EICEs)[23]. Assembly of the PU.1-EICE complex requires phosphorylation of PU.1 at Ser148. Because EICE are present in interferon promoters, we tested whether ELF4 enhances the binding of IRF3 or IRF7 to the interferon promoters and synergizes with IRFs for interferon expression. Overexpressed ELF4 synergized with IRF3 to activate the *Ifnb1* promoter in 293T cells (**Supplementary Fig. 6c**). We found a single GGAA motif in the *Ifna4* promoter that is mainly activated by IRF7. We next tested the effect of ELF4 on IRF7-mediated activation of the *Ifna4* reporter. ELF4 overexpression alone did not activate the *Ifna4* reporter (**Supplementary Fig. 1e**), whereas overexpression of IRF7 alone resulted in a 20-fold induction of IFN-α4–Luc reporter activity (**Fig. 7f**). Co-expression of ELF4 strongly enhanced IRF7 transactivation activity in a dose-dependent manner (up to 150-fold; **Fig. 7f** and **Supplementary Fig. 6g**). In contrast, ELF4 has minimal effect on the IRF7-mediated activation of a ISRE-Luc reporter (**Supplementary Fig. 6h,i**).

To determine the physiological function of ELF4 in regulating IRF3-IRF7 and NF-κB activity, we performed ChIP-qPCR in untreated or VSV-infected wild-type or ELF4-deficient peritoneal macrophages (**Fig. 7e,g**). VSV-induced recruitment of IRF3 and p65 to the *Ifnb1* promoter was significantly reduced in *Elf4*$^{-/-}$ macrophages (**Fig. 7e**). Similarly,

the binding of IRF7 to the *Ifna4* promoter was decreased in *Elf4*$^{-/-}$ macrophages (**Fig. 7g**). Furthermore, we observed cooperative binding of ELF4 and IRF–NF-κB to IFN-β in EMSA (**Supplementary Fig. 6j**). The EICE element of the *Ifnb1* promoter was indispensable for the cooperative transactivation mediated by ELF4, IRF3 and p65, indicating an EICE-dependent formation of ELF4-IRF complex (**Fig. 7h**). Comparative kinetic analyses showed parallel virus-induced activation of ELF4, NF-κB and IRF-3 MEFs (**Fig. 7i**). Similar to the expression of IRF7, ELF4 expression was low in most tissues (**Supplementary Fig. 7a**). We noted comparable reduction in the production *Ifnb1* and *Isg15* in *Elf4*$^{-/-}$ and *Irf3*$^{-/-}$ MEFs (**Supplementary Fig. 7b,c**). Taken together, our data indicate that ELF4 is important for the recruitment of IRF3, IRF7 and p65 to interferon promoters and for the induction of interferon gene expression.

DISCUSSION

Many ETS domain–containing proteins are targets of signal transduction pathways and are activated in response to a wide array of extra-cellular stimuli. We demonstrated that ELF4 was induced after viral infection and interferon treatment, and upregulated production of type I interferon in a feed-forward loop. Genetic deletion of ELF4 rendered mice highly susceptible to WNV infection. Analysis of *Elf4*$^{-/-}$ macrophages, DCs and MEFs revealed that ELF4 was essential for efficient production of type I interferons. ELF4 was downstream the adaptor proteins TRIF, MyD88, STING and MAVS and was phosphorylated by TBK1. As is the case with p65 (ref. 39), ectopic expression of ELF4 was constitutively active and resulted in formation of dimers. We speculate that overexpressed ELF4 may recruit and be activated by TBK1. Overexpressed ELF4 bypassed upstream signals and induced type I interferon in the absence of these adaptor proteins. In *Tbk1*$^{-/-}$ cells, overexpressed ELF4 was inactive, as phosphorylation did not occur. ELF4 cooperated with IRF3, IRF7 or p65 to bind to ELF4-IRF or ELF4–NF-κB composite motifs in type I interferon promoters and to activate interferon gene expression.

Rapid induction of type I interferon expression is a central event in establishing the innate antiviral response. Molecular regulation of interferon gene expression is tightly regulated by extracellular and intracellular signals generated during primary infection and culminates in the activation of NF-κB and IRFs. These in turn trigger an immediate early interferon response characterized by the release of IFN-β and IFN-α1. IRF3 and IRF7 have essential roles in virus-induced production of type I interferon[40]. IRF3 is constitutively expressed and is crucial for the initial induction of immediate early genes such as those encoding IFN-β, IFN-α1 and CCL5 (ref. 14). In contrast, IRF7 is synthesized *de novo* upon interferon stimulation and contributes to the expression of delayed-type genes including other interferon subtypes[36]. Similarly to the expression of IRF7, ELF4 expression is low in most tissues and is induced by type I interferons, suggesting a major role in the subsequent feed-forward amplification of interferons. Like IRF3 and IRF7, ELF4 is phosphorylated after viral infection. Thus, in many respects, ELF4 has a mode of expression and activation similar to that of IRF7. Moreover, we noted comparable reduction in the production type I interferon in *Elf4*$^{-/-}$ and *Irf3*$^{-/-}$ MEFs. Thus, ELF4 is a newly recognized and distinct IRF that has functional similarity with IRF3 and IRF7. In addition to IRF3 and IRF7, recent studies have shown that IRF5 contributes to activation of type I interferon in myeloid DCs[41]. Induciton of IFN-β was impaired in *Elf4*$^{-/-}$ BMDCs in response to TLR and RLR agonists, suggesting that cooperative binding of IRF5 and ELF4 to the *Ifnb1* promoter may exist in myeloid DCs.

In common with many other transcription factors, ETS proteins exhibit low selectivity in binding-site preference, which suggests that the specificity of promoter targeting by ETS proteins relies on cooperation with transcription factors. Indeed, combinatorial control is a

characteristic property of the ETS family, which involves interaction between ETS members and other key transcription factors such as SRF, Pax, AP1, IRF and NF-κB family members[42–44]. In response to parathyroid hormone, ELF4 is phosphorylated by JNK. JNK activates the oncoprotein c-Jun, thereby forming the activator protein-1 (AP-1) transcription factor as a homodimer or heterodimer[45].

ETS proteins are a family of multifunctional transcription factors that direct gene expression by binding to target genes carrying specific consensus GGAA DNA-binding recognition sites. The IRFs regulate expression of target genes by binding to an ISRE that usually contains a potential ETS-binding site (GGAA)[23]. A cooperative correlation between ETS proteins and IRFs has been described[23]. PU.1 can interact with IRF2, IRF4 and IRF8 to form a heterodimeric complex in its target gene promoters and thereby regulate gene transcription. We here identified and characterized an ETS protein ELF4 as an interferon transcription factor that enhances the DNA-binding affinity of IRF3 and IRF7. We did not observe a direct protein interaction between ELF4 and IRF3 or IRF7 (data not shown) suggesting that protein-protein interaction is not essential for cooperative binding to the promoters[46]. Instead, cooperation arises mainly through co-binding of transcription factors dependent on nucleotide sequence (ETS-binding motif and ISRE). We found a new enhancer box (E-box), EICE, in interferon promoters. Thus ELF4 synergizes with IRF3, IRF7 and NF-κB to induce type I interferons by cooperative binding of these transcription factors via the ETS binding motif. As both ETS proteins and IRFs are widely expressed and participate in many important biological processes, the characterization of EICE may contribute to understanding gene regulation in diverse fields, including innate immunity.

In conclusion, ELF4 is a new type I IRF that activates the innate immune response by promoting the production of type I interferons, which are critical for immune surveillance of different classes of viral pathogens. Exploiting or enhancing ELF4-mediated signaling may lead to new strategies for combatting infectious diseases; conversely, inhibiting ELF4 may result in immunosuppression.

ONLINE METHODS

Mice, cells, human macrophages, viruses, antibodies and reagents

Elf4$^{-/-}$ mice on a C57BL/6J background have been described previously[29]. *Sting*$^{gt/gt}$ mice, which lack a functional STING protein, were a gift from R. Vance (University of California, Berkeley). *Irf3*$^{-/-}$ mice were a gift from R. Medzhitov (Yale University), *Myd88*$^{-/-}$ mice were a gift from R. Flavell (Yale University). 293T, HeLa, L929 (mouse fibroblast cells), 2fTGH-ISRE (human fibrosarcoma cells expressing an ISRE), L929-ISRE and Vero cells were cultured in DMEM. Isolation of MEFs, BMDMs and macrophages was performed as described[12]. BMDCs were isolated from tibia and femur. Cells were cultured in 10-cm Petri-dish at 37 °C for 5 d. The medium for BMDCs was RPMI-1640 medium containing GM-CSF at 100 U/ml and TNF at 50 U/ml. 293-hTLR4A-MD2-CD14 and 293XL-hTLR7 cells were from InvivoGen. Heparinized human blood was obtained with written informed consent from healthy donors, and primary macrophages were derived from peripheral blood monocytes and infected with WNV as described[47]. VSVGFP (Indiana strain) was a gift from J. Rose (Yale University), and HSV-1 was from A. Iwasaki (Yale University). SeV (Cantell strain; VR-907) and EMCV (VR-129B) were purchased from American Type Culture Collection (ATCC). Single-cycle HIV virus was prepared by cotransfecting 293 cells with VSV-G (0.07 μg) or YU2 (1.33 μg), pOPRIgagpol (1.5 μg), Ps-ReV(0.33 μg) and HIVec2GFP (0.66 μg). Poly(I:C) (catalog number tlr-pic), poly(I: C)-LMW (tlr-picw), flagellin (tlrl-bsfla), lipoteichoic acid (LTA; tlrl-lta), R848 (tlrl-r848), Pam3CSK4 (tlrl-pms) and CpG oligonucleotide (tlr-1585) were from Invivogen. LPS (L4391) was from Sigma. Poly(dA-dT) was synthesized as 5′-d(AT)30-3′ and was annealed by heating to 95 °C and

cooling to 25 °C. Lipofectamine 2000 (Invitrogen) and TransIT-LT1 (MIR2300, Mirus) was used for lipid transfection. The following antibodies were used: anti-ELF4 (ELF4) (AV38028), anti-Flag (F3165), anti-GAPDH (G8795), anti-HA (H3663) and anti-VSV (A5977; all from Sigma); anti-phospho-IRF3 (Ser396; Cell Signaling) anti-IRF3 (D83B9) and; anti-MAVS (sc-68881 (Santa Cruz) and 3993 (Cell Signaling)); and anti–histone H3 (31560; Upstate). Anti-Sendai virus polyclonal antibody (PD029) was from MBL. The antibodies were diluted 1,000 times for immunoblots, 200 times in immunofluorescence and ChIP assay. Human interferon beta (C11420-1) was from PBL interferon. The IFN-β ELISA kits were obtained from PBL.

Approval and consent for experiments

The work described in this paper involves studies in experimental animals. All relevant, institutional approvals were obtained (protocol number: 2010-10404, Yale University's Institutional Animal Care and Use Committee). Heparinized blood from healthy volunteers was obtained with written informed consent under an approved protocol of the Human Investigations Committee of Yale University School of Medicine. Informed consent was obtained from all subjects. The sample size was chosen based on power analysis. We did not exclude any samples. No randomization or blinding was done. We tested and authenticated the cell lines for myco-plasma contamination.

Reporter analysis

293T cells seeded on 24-well plates were transiently transfected with 50 ng of the luciferase reporter plasmid together with a total of 600 ng of various expression plasmids or empty control plasmids. As an internal control, 10 ng of pRL-TK was transfected simultaneously. Dual luciferase activity in the total cell lysates was quantified 24–36 h after transfection.

Immunofluorescence confocal microscopy

These experiments were performed as described[12] with cell imaging using an Olympus BX51 microscope or a Leica TCS SP2 confocal system under a 25× objective.

Type I interferon bioassay

The activity of type I interferon and TNF was measured as described[25], with reference to recombinant human or mouse IFN-β (R&D Systems) as a standard with 2fTGH cells stably transfected with an interferon-sensitive (ISRE) luciferase construct.

Plaque assay

The VSV plaque assay was performed as described[48]. For the HSV-1 and WNV plaque assays ~1×10^5 cells were infected with virus, and 24 h later supernatants were collected and used to infect confluent Vero cells. After a 1-h incubation, supernatants were removed, and cells were washed with PBS, culture medium containing 2% (wt/vol) methylcellulose was overlaid for 60 h, cells were fixed for 30 min with 0.5% (vol/vol) glutaraldehyde and then stained with 1% (wt/vol) crystal violet dissolved in 70% ethanol. Plaques were counted, and average counts were multiplied by the dilution factor to determine the viral titer as plaque-forming units per milliliter.

Co-immunoprecipitation, immunoblot analysis and native PAGE

These procedures were performed as described[13]. For endogenous coimmunoprecipitation, cells (2×10^7) were lysed in 1 ml of lysis buffer, and subsequent procedures were done as described[13].

Nuclear-cytoplasmic fractionation

293 cells were transfected with plasmids encoding ELF4 or MAVS, or infected with SeV and harvested after 20 h. Nuclear-cytoplasmic fractionation was conducted using the NE-PER Nuclear and Cytoplasmic Extraction Reagents kit (Thermo Fisher Scientific) according to the manufacturer's protocol.

Flow cytometry analysis

293T cells, HeLa cells, MEFs and macrophages were infected with VSV-GFP and harvested at the indicated time. Cells were fixed by intracellular fixation buffer (00-8222-49, eBioscience) and analyzed by FACS Calibur (BD Biosciences).

Quantitative real-time PCR

Total RNA was isolated from cells using the RNeasy RNA extraction kit (Qiagen), and cDNA synthesis was performed using 1 μg of total RNA (iScriptcDNA Synthesis kit). qPCR was done with gene-specific primers and 6FAM-TAMRA (6-carboxyfluorescein–N,N,N′,N′-tetramethyl-6-carboxyrhodamine) probes or inventoried gene expression kits from Applied Biosystems (6FAM-MGB (6-carboxyfluorescein minor-groove binder) probes).

Chromatin immunoprecipitation

ChIP was conducted using Magna Chip A/G (Millipore). *Ifnb1*and *Ifna2* promoter primers are listed in **Supplementary Table 3**. ChIP samples were analyzed by real-time qPCR with the SYBR-Green Master Mix system (Bio-Rad).

L929 bioassay

Levels of biologically active interferon in serum were measured using an EMCV L929 cytopathic effect bioassay as described[49]. Results were compared with a standard curve using recombinant mouse IFN-α (PBL Laboratories).

Electrophoretic mobility shift assay

Oligonucleotides for the EMSA were amplified with either a biotin-labeled or unlabeled primer using the wild-type and mutant IFN-β–Luc as template, and purified by Qiagen PCR kits. EMSAs were performed by incubating 0.5 ng of labeled probe with nuclear extract or purified protein (10 μg) and competing oligonucleotides in binding buffer (10 mM Tris-HCl, pH 7.5, 50 mM NaCl, 1 mM dithiothreitol, 1 mM EDTA, 5% glycerol and 1 μg/μl poly(dI·dC) at room temperature for 30 min. Mixtures were size-fractionated on a nondenaturing 4% polyacrylamide gel followed by transfer to nitrocellulose membranes and detected using streptavidin-HRP chemiluminescence for biotin-labeled probes (Light Shift Chemiluminescent EMSA Kit; Pierce).

Kinase assay

PCDNA 3.1PCBP2, ELF4 and STING were expressed *in vitro* using TnT T7 Quick Coupled Transcription-Translation System (Promega, L1170). The kinase activity was analyzed by TBK1 kinase enzyme system and ADP-Glo assay (Promega, V8291).

Reconstitution of mice with NK cells and NKT cells

NK or NKT cells were isolated from splenocytes of wild-type mice using NK cell isolation kit II (Miltenyi Biotec, 130-096-892) or NK1.1+ iNKT cell isolation kit (Miltenyi Biotec, 130-096-513). Purity of isolated cells was >95% upon analysis by flow cytometry. 1×10^6 cells NK cells and 1×10^6 NKT cells were injected intravenously into recipient mice.

RNA interference

ELF4 siRNA (catalog number: SASI_Hs01_00189458, SASI_Hs01_00189459, SASI_Hs01_00189460), IRF3 siRNA (catalog number: SASI_Hs02_00332144, SASI_Hs02_00332145), TRIF siRNA (catalog number: SASI_Hs01_00226929, SASI_Hs01_00226930, SASI_Hs01_00226931), MyD88 siRNA (catalog number: SASI_Hs01_00111539, SASI_Hs01_00111540, SASI_ Hs01_00111541), STING siRNA (catalog number: SASI_Hs02_00371843, SASI_Hs01_00031029, SASI_Hs01_00031030), MAVS siRNA (catalog number: SASI_Hs01_00128708, SASI_Hs01_00128711) and scrambled siRNA (catalog number: SASI_Hs01_00224995) were purchased from Sigma. RelA siRNA (catalog number: SR304030A, SR304030B, SR304030C) and scrambled siRNA were from Origene. TBK1 siRNA (catalog number: cs-39058) was from Santa Cruz.

Transfection of primary MEF cells

Primary MEF cells were transfected using mouse/rat nucleofector solution (Lonza, M-FB-481) and nucleofector II system.

Plasmids

'Pcmv5-humanELF4' has been described previously[34], and the sequence encoding full-length ELF4 was subcloned to Pcmv7.1 and Pcmv3xHA vectors. Deleted, truncated and point mutants of ELF4 were generated by the QuickChange site-directed mutagenesis kits (Stratagene) and the construct encoding wild-type protein as the template (**Supplementary Table 3**). Each mutation was confirmed by sequencing. After cDNA encoding human ELF1, ELF2, ELF3, ELF5 or mouse ELF4 was amplified from cDNA made from 293, U937 or L929 cells, it was cloned into plasmid p3xFLAG-CMV-7.1 (Sigma), pCMV-3XHA or pcDNA3.1(+)-3′VSV (Invitrogen) to generate plasmids encoding Flag-tagged, HA-tagged or VSV-tagged protein, respectively. pCMV4-p50(21965) and pCMV4-p65(21966) are from Addgene. The plasmids encoding human STING, MAVS, TBK1, IRF3, IRF7 and STK38 have been described[28]. For reporter assays, pISRE-Luc (Stratagene) and pNifty-Luc (Invivogen), an NF-κB–dependent E-selectin luciferase reporter plasmid, were used. Other promoters were cloned into pGL3-Basic vector (Promega) with the following promoter regions: −1 to −155 for mouse *Ifnb1*, and −1 to −476 for mouse *Ifna4*. All constructs were verified by sequencing the relevant regions. Point mutants of IFN-β reporter were generated by the QuickChange site-directed mutagenesis kits (Stratagene), and the construct encoding wild-type IFN-β–Luc as the template (**Supplementary Table 3**). Each mutation was confirmed by DNA sequencing.

Statistical analysis

Student's *t*-test, log-rank test and nonparametric Mann-Whitney analysis were used to analyze data. Data are presented are means ± s.e.m. unless otherwise noted, and experiments were repeated at least three times. Results were considered significant at $P < 0.05$.

Supplementary Material

Refer to Web version on PubMed Central for supplementary material.

Acknowledgments

We thank S. Nimer (University of Miami) for the *Elf4*$^{-/-}$ mice, Z. Jiang (Peking University) for the reporter plasmids. This work was supported by the US National Institutes of Health (N01-HHSN272201100019C, AI099625 and AI08992). E.F. and A.I. are funded by the Howard Hughes Medical Institute.

References

1. Takeuchi O, Akira S. Innate immunity to virus infection. Immunol. Rev. 2009; 227:75–86. [PubMed: 19120477]
2. Liew FY, Xu D, Brint EK, O'Neill LA. Negative regulation of toll-like receptor-mediated immune responses. Nat. Rev. Immunol. 2005; 5:446–458. [PubMed: 15928677]
3. Kawai T, et al. IPS-1, an adaptor triggering RIG-I- and Mda5-mediated type I interferon induction. Nat. Immunol. 2005; 6:981–988. [PubMed: 16127453]
4. Meylan E, et al. Cardif is an adaptor protein in the RIG-I antiviral pathway and is targeted by hepatitis C virus. Nature. 2005; 437:1167–1172. [PubMed: 16177806]
5. Seth RB, Sun L, Ea CK, Chen ZJ. Identification and characterization of MAVS, a mitochondrial antiviral signaling protein that activates NF-κB and IRF 3. Cell. 2005; 122:669–682. [PubMed: 16125763]
6. Xu LG, et al. VISA is an adapter protein required for virus-triggered IFN-beta signaling. Mol. Cell. 2005; 19:727–740. [PubMed: 16153868]
7. Barber GN. Cytoplasmic DNA innate immune pathways. Immunol. Rev. 2011; 243:99–108. [PubMed: 21884170]
8. Chiu YH, Macmillan JB, Chen ZJ. RNA polymerase III detects cytosolic DNA and induces type I interferons through the RIG-I pathway. Cell. 2009; 138:576–591. [PubMed: 19631370]
9. Unterholzner L, et al. IFI16 is an innate immune sensor for intracellular DNA. Nat. Immunol. 2010; 11:997–1004. [PubMed: 20890285]
10. Parvatiyar K, et al. The helicase DDX41 recognizes the bacterial secondary messengers cyclic di-GMP and cyclic di-AMP to activate a type I interferon immune response. Nat. Immunol. 2012; 13:1155–1161. [PubMed: 23142775]
11. Sun L, Wu J, Du F, Chen X, Chen ZJ. Cyclic GMP-AMP synthase is a cytosolic DNA sensor that activates the type I interferon pathway. Science. 2013; 339:786–791. [PubMed: 23258413]
12. Ishikawa H, Barber GN. STING is an endoplasmic reticulum adaptor that facilitates innate immune signalling. Nature. 2008; 455:674–678. [PubMed: 18724357]
13. Sun W, et al. ERIS, an endoplasmic reticulum IFN stimulator, activates innate immune signaling through dimerization. Proc. Natl. Acad. Sci. USA. 2009; 106:8653–8658.
14. Zhong B, et al. The adaptor protein MITA links virus-sensing receptors to IRF3 transcription factor activation. Immunity. 2008; 29:538–550. [PubMed: 18818105]
15. Chen H, et al. Activation of STAT6 by STING is critical for antiviral innate immunity. Cell. 2011; 147:436–446. [PubMed: 22000020]
16. Daffis S, Suthar MS, Szretter KJ, Gale M Jr. Diamond MS. Induction of IFN-beta and the innate antiviral response in myeloid cells occurs through an IPS-1-dependent signal that does not require IRF-3 and IRF-7. PLoS Pathog. 2009; 5:e1000607. [PubMed: 19798431]
17. Yamada T, Park CS, Mamonkin M, Lacorazza HD. Transcription factor ELF4 controls the proliferation and homing of CD8+ T cells via the Kruppel-like factors KLF4 and KLF2. Nat. Immunol. 2009; 10:618–626. [PubMed: 19412182]
18. Sashida G, et al. ELF4/MEF activates MDM2 expression and blocks oncogene-induced p16 activation to promote transformation. Mol. Cell Biol. 2009; 29:3687–3699. [PubMed: 19380490]
19. Meadows SM, Myers CT, Krieg PA. Regulation of endothelial cell development by ETS transcription factors. Semin. Cell Dev. Biol. 2011; 22:976–984. [PubMed: 21945894]
20. Sivina M, et al. The transcription factor E74-like factor controls quiescence of endothelial cells and their resistance to myeloablative treatments in bone marrow. Arterioscler. Thromb. Vasc. Biol. 2011; 31:1185–1191. [PubMed: 21350194]
21. Yao JJ, et al. Tumor promoting properties of the ETS protein MEF in ovarian cancer. Oncogene. 2007; 26:4032–4037. [PubMed: 17213815]
22. Mao S, Frank RC, Zhang J, Miyazaki Y, Nimer SD. Functional and physical interactions between AML1 proteins and an ETS protein, MEF: implications for the pathogenesis of t(8;21)-positive leukemias. Mol. Cell Biol. 1999; 19:3635–3644. [PubMed: 10207087]

23. Gobin SJ, Biesta P, Van den Elsen PJ. Regulation of human beta 2-microglobulin transactivation in hematopoietic cells. Blood. 2003; 101:3058–3064. [PubMed: 12480693]
24. Sauer JD, et al. The N-ethyl-N-nitrosourea-induced Goldenticket mouse mutant reveals an essential function of Sting in the in vivo interferon response to Listeria monocytogenes and cyclic dinucleotides. Infect. Immun. 2011; 79:688–694. [PubMed: 21098106]
25. You F, et al. PCBP2 mediates degradation of the adaptor MAVS via the HECT ubiquitin ligase AIP4. Nat. Immunol. 2009; 10:1300–1308. [PubMed: 19881509]
26. Suico MA, et al. Functional dissection of the ETS transcription factor MEF. Biochim. Biophys. Acta. 2002; 1577:113–120. [PubMed: 12151102]
27. Suthar MS, et al. IPS-1 is essential for the control of West Nile virus infection and immunity. PLoS Pathog. 2010; 6:e1000757. [PubMed: 20140199]
28. Wang T, et al. Toll-like receptor 3 mediates West Nile virus entry into the brain causing lethal encephalitis. Nat. Med. 2004; 10:1366–1373. [PubMed: 15558055]
29. Lacorazza HD, et al. The ETS protein MEF plays a critical role in perforin gene expression and the development of natural killer and NK-T cells. Immunity. 2002; 17:437–449. [PubMed: 12387738]
30. Diamond MS, Shrestha B, Mehlhop E, Sitati E, Engle M. Innate and adaptive immune responses determine protection against disseminated infection by West Nile encephalitis virus. Viral Immunol. 2003; 16:259–278. [PubMed: 14583143]
31. Vargin VV, Semenov BF. Changes of natural killer cell activity in different mouse lines by acute and asymptomatic flavivirus infections. Acta Virol. 1986; 30:303–308. [PubMed: 2876611]
32. Shrestha B, Diamond MS. Role of CD8+ T cells in control of West Nile virus infection. J. Virol. 2004; 78:8312–8321. [PubMed: 15254203]
33. Tough DF. Modulation of T-cell function by type I interferon. Immunol. Cell Biol. 2012; 90:492–497. [PubMed: 22391814]
34. Yokoyama M, et al. Inducible histamine protects mice from P. acnes-primed and LPS-induced hepatitis through H2-receptor stimulation. Gastroenterology. 2004; 127:892–902. [PubMed: 15362044]
35. Miyahira AK, Shahangian A, Hwang S, Sun R, Cheng G. TANK-binding kinase-1 plays an important role during in vitro and in vivo type I IFN responses to DNA virus infections. J. Immunol. 2009; 182:2248–2257. [PubMed: 19201879]
36. Wei GH, et al. Genome-wide analysis of ETS-family DNA-binding in vitro and in vivo. EMBO J. 2010; 29:2147–2160. [PubMed: 20517297]
37. Nolan GP. NF-AT-AP-1 and Rel-bZIP: hybrid vigor and binding under the influence. Cell. 1994; 77:795–798. [PubMed: 8004669]
38. Bonnefoy E, Bandu MT, Doly J. Specific binding of high-mobility-group I (HMGI) protein and histone H1 to the upstream AT-rich region of the murine beta interferon promoter: HMGI protein acts as a potential antirepressor of the promoter. Mol. Cell Biol. 1999; 19:2803–2816. [PubMed: 10082546]
39. Collett GP, Campbell FC. Overexpression of p65/RelA potentiates curcumin-induced apoptosis in HCT116 human colon cancer cells. Carcinogenesis. 2006; 27:1285–1291. [PubMed: 16497702]
40. Sato M, et al. Distinct and essential roles of transcription factors IRF-3 and IRF-7 in response to viruses for IFN-alpha/beta gene induction. Immunity. 2000; 13:539–548. [PubMed: 11070172]
41. Lazear HM, et al. IRF-3, IRF-5, and IRF-7 coordinately regulate the type I IFN response in myeloid dendritic cells downstream of MAVS signaling. PLoS Pathog. 2013; 9:e1003118. [PubMed: 23300459]
42. Verger A, Duterque-Coquillaud M. When Ets transcription factors meet their partners. BioEssays. 2002; 24:362–370. [PubMed: 11948622]
43. Tussiwand R, et al. Compensatory dendritic cell development mediated by BATF-IRF interactions. Nature. 2012; 490:502–507. [PubMed: 22992524]
44. Glasmacher E, et al. A genomic regulatory element that directs assembly and function of immune-specific AP-1-IRF complexes. Science. 2012; 338:975–980. [PubMed: 22983707]

45. Papachristou DJ, Batistatou A, Sykiotis GP, Varakis I, Papavassiliou AG. Activation of the JNK-AP-1 signal transduction pathway is associated with pathogenesis and progression of human osteosarcomas. Bone. 2003; 32:364–371. [PubMed: 12689679]

46. Panne D, Maniatis T, Harrison SC. Crystal structure of ATF-2/c-Jun and IRF-3 bound to the interferon-beta enhancer. EMBO J. 2004; 23:4384–4393. [PubMed: 15510218]

47. Kong KF, et al. Dysregulation of TLR3 impairs the innate immune response to West Nile virus in the elderly. J. Virol. 2008; 82:7613–7623. [PubMed: 18508883]

48. Wang P, et al. Caspase-12 controls West Nile virus infection via the viral RNA receptor RIG-I. Nat. Immunol. 2010; 11:912–919. [PubMed: 20818395]

49. Samuel MA, et al. PKR and RNase L contribute to protection against lethal West Nile virus infection by controlling early viral spread in the periphery and replication in neurons. J. Virol. 2006; 80:7009–7019. [PubMed: 16809306]

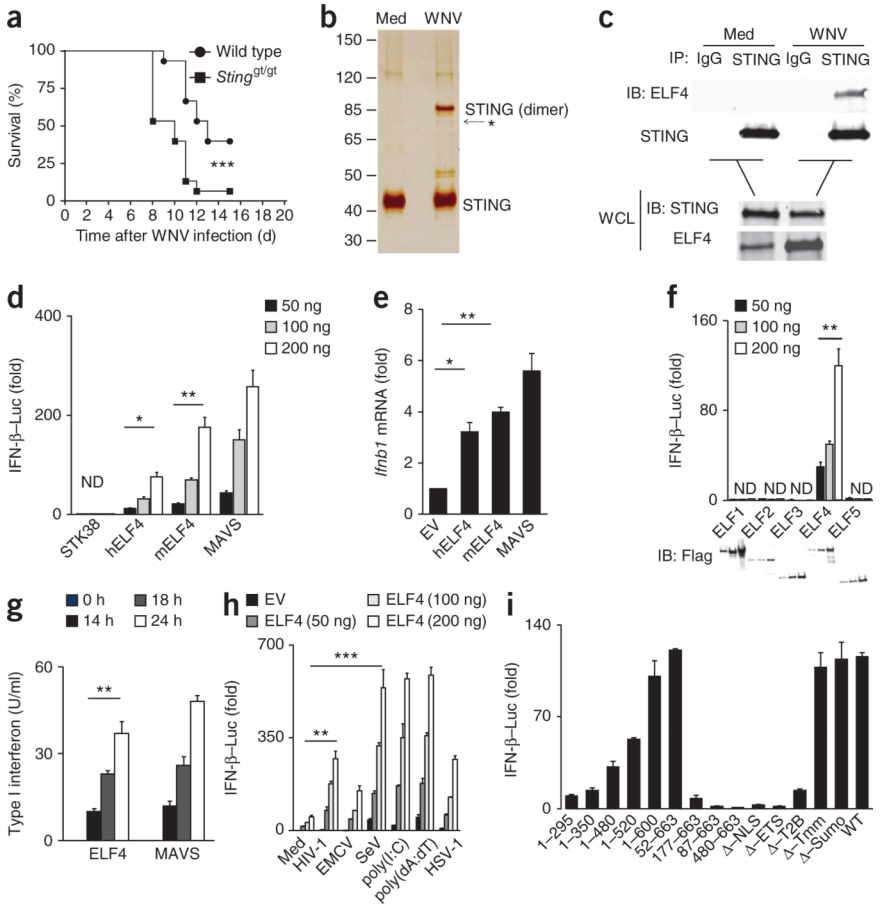

Figure 1.

ELF4 is an interferon stimulator and binds to STING. (**a**) Survival of age- and sex-matched wild-type mice (C57BL/6) and *Sting*$^{gt/gt}$ mice inoculated subcutaneously (n = 14 mice per group) with 200 plaque-forming units of WNV and monitored daily for 15 d. ***P = 0.009 (log-rank test). (**b**) SDS-PAGE of HeLa cells expressing Flag-ELF4 treated with WNV (multiplicity of infection of 1) or medium (Med) and harvested 4 h after infection followed by immunoprecipitation using anti-Flag antibody. *, ELF4 identified by mass spectrometry. (**c**) Immunoblot (IB) of HeLa cells that were infected with WNV for 6 h, lysed and immunoprecipitated (IP) with anti-STING or control IgG. Whole cell lysates (WCL) were immunoblotted with antibodies to indicated proteins. (**d**) Luciferase activity of IFN-β in 293T cells 24 h after transfection with an IFN-β–Luc plasmid and 50 ng, 100 ng or 200 ng of plasmids encoding human ELF4 (hELF4), mouse ELF4 (mELF4), MAVS or STK38. (**e**) qRT-PCR analysis of *Ifnb* mRNA (normalized to β-actin) in MEFs transfected with empty vector (EV) or plasmids encoding indicated proteins. (**f**) Luciferase assay (top) and immunoblot analysis (bottom) of 293T cells transfected with an IFN-β–Luc plasmid and indicated amounts of ELFs. (**g**) Relative luciferase readout (compared to actin), translated to interferon concentrations by standard curve, from 293T cells transfected with ELF4 or MAVS plasmids, from which 24 h later, the supernatants were transferred to 2fTGH-ISRE-Luc cells, and in which 6 h later luciferase activity was measured. (**h**) Luciferase activity in 293T cells transfected with IFNβ-Luc plasmid and empty vector (EV) or indicated amounts of ELF4 plasmid and 24 h later infected with viruses, or transfected with poly(I:C) or poly(dA:dT). (**i**) Luciferase activity analyzed as in **d** in 293T cells transfected with plasmids (100 ng) encoding fragments of ELF4 of indicated lengths, Δ-NLS (ELF4 without the

nuclear localization sequence), Δ-ETS (ELF4 without the ETS domain), Δ-T2B (ELF4 without TRAF2 binding domain), Δ-Tmm (ELF4 without transmembrane domain), Δ-Sumo (ELF4 without sumoylation site). ND, none detected. $^{**}P < 0.01$ and $^{***}P < 0.001$ (Student's *t*-test; **d–i**). Data were pooled from two (**a–c**) or three (**d–i**) independent experiments. Error bars, s.e.m.; $n = 3$ cultures (**d–i**).

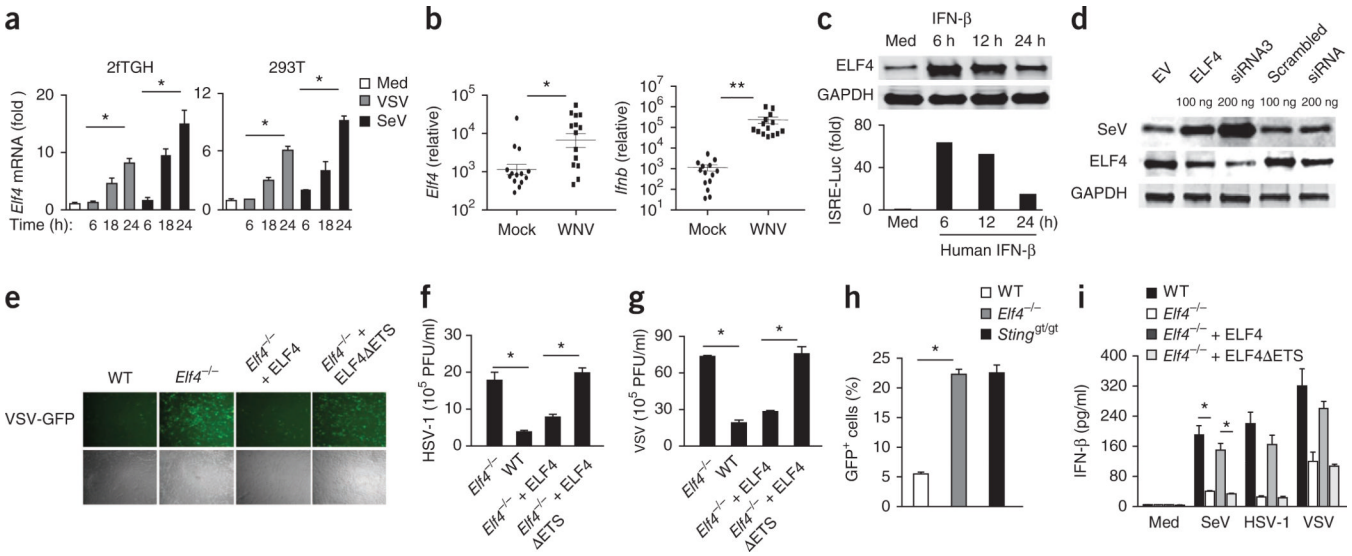

Figure 2.

ELF4 is involved in the antiviral immune signaling. (**a**) qRT-PCR analysis of *Elf4* mRNA (normalized to β-actin) in 2fTGH and 293T cells in medium (Med) and after infection with SeV or VSV. **P* (**b**) qRT-PCR analysis of *Elf4* and *Ifnb1* mRNA (normalized to β-actin) in primary monocyte–derived macrophages from human donors 12 h after infection with WNV. **P* < 0.01 and ***P* < 0.0001 (nonparametric Mann-Whitney analysis). (**c**) Immunoblot of 2fTGH cells after treatment with human IFN-β (100 units/ml) at the indicated times and fold-induction assessed using the luciferase assay. (**d**) Immunoblot with antibodies to indicated proteins in 293T cell lysates after transfection with 100 ng or 200 ng of scrambled or ELF4-specific siRNA and infection with SeV for 24 h. EV, empty vector. RNAi3 is described in **Supplementary Figure 3**. (**e–g,i**) Microscopy analysis (**e**; magnification, 5×), plaque-formation assays (**f,g**) and enzyme-linked immunosorbent assay (i) in *Elf4*$^{-/-}$ MEFs expressing wild-type ELF4 or variants lacking the ETS domain along with wild-type MEFs and untransfected cells after 24 h infection with VSV-GFP, SeV or HSV-1. (**h**) Flow cytometry analysis in wild-type, *Sting*$^{gt/gt}$ or *Elf4*$^{-/-}$ peritoneal macrophages after 24 h infection with VSV-GFP. **P* < 0.01 (Student's *t*-test; **a,f–i**). Data were pooled from two (**c–e**) or three (**a,b,f–i**) independent experiments. Error bars, s.e.m.; *n* = 3 cultures (**a,f–i**) and *n* = 14 samples (**b**).

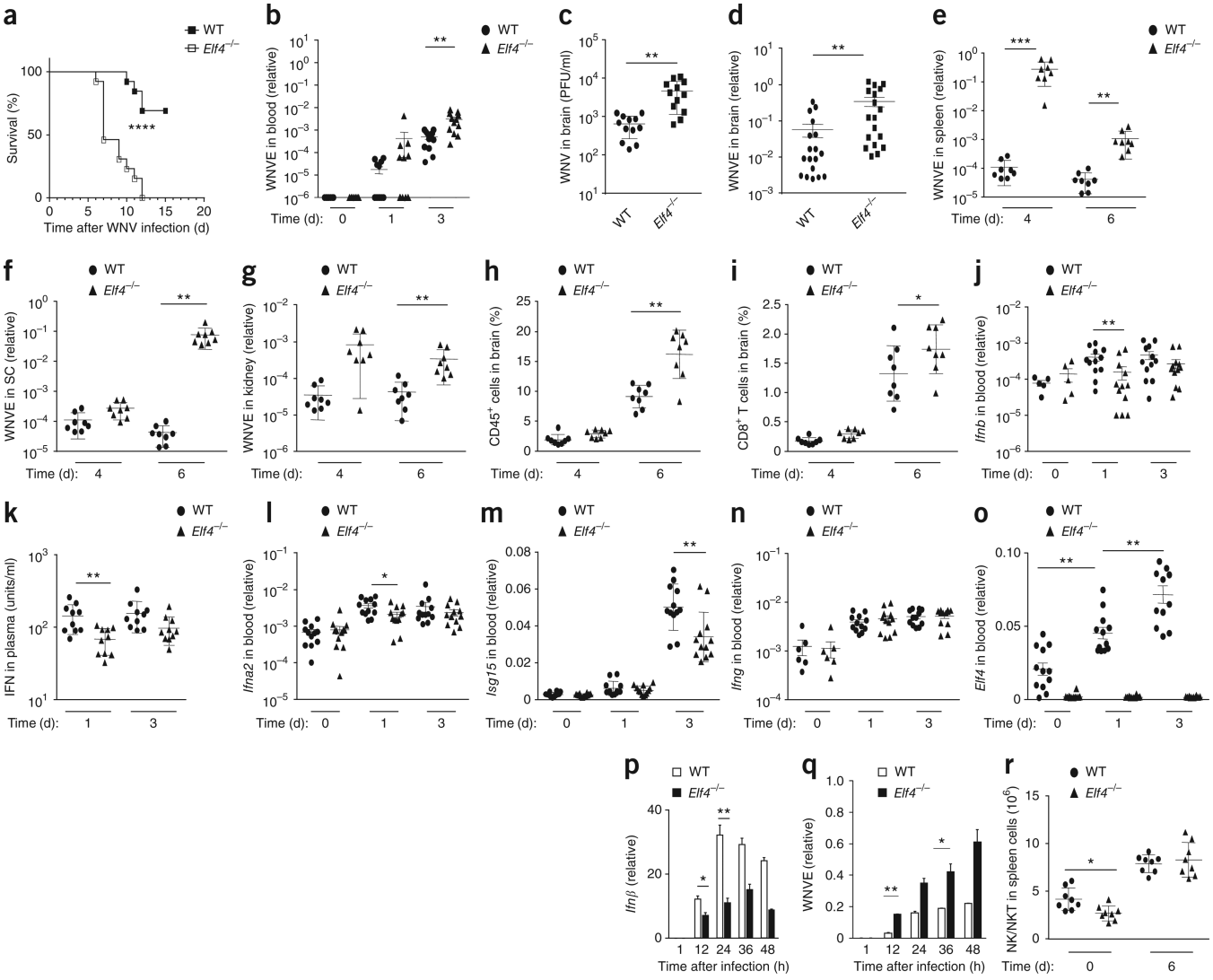

Figure 3.

ELF4 is critical for antiviral immunity *in vivo*. (**a**) Mortality of age- and sex-matched wild-type (WT; C57BL/6) and *Elf4*$^{-/-}$ mice inoculated subcutaneously with 200 plaque-forming units of WNV and monitored daily for 15 d. (**b–d**) qRT-PCR analysis normalized to β-actin expression and plaque assay showing viral loads in the blood of mice at day 0, 1 or 3 (**b**), in the brains of mice at day 8 (**c,d**) after infection with WNV. (**e–g**) Viral loads in the spleen, spinal cord (SC) and kidney of mice on day 4 or day 6 after infection with WNV, assessed by qRT-PCR analysis of WNVE and plaque assay. (h,i) Flow cytometry analysis of CD45^{+} cells and CD8^{+} T cells in brain of the mice on day 0 and day 6 after infection with WNV. (**j,l–o**) qRT-PCR analysis of *Ifnb1* (**j**), *Ifna2* (**l**), *Isg15* (**m**), *Ifng* (**n**) and *Elf4* (**o**) transcripts, normalized to β-actin, in blood cells from mice at day 0, 1 and 3 after infection with WNV. (**k**) Abundance of type I interferon measured by EMCV bioassay in the plasma from mice at days 1 and 3 after infection with WNV. (**p,q**) qRT-PCR analysis of *Ifnb1* and WNVE mRNA in wild type or *Elf4*$^{-/-}$ peritoneal macrophages 24 h after infection with WNV. (r) Flow cytometry analysis of NK cells in spleen of the mice at day 0 and day 6 after subcutaneous infection with WNV. ****$P = 0.0001$ (**a**; log-rank test). *$P < 0.05$ and **$P < 0.01$ (Student's *t*-test; **p,q**); *$P < 0.05$ and **$P < 0.01$ (nonparametric Mann-Whitney analysis for all data except **a,p,q**). Data were pooled from two (**p,q**) or three (**a–o,r**)

independent experiments. Error bars, s.e.m. (n = 8 mice per group (**h,i,r**), n = 12 mice per group (**b–g,j–o,r**) and n = 3 cultures (**p,q**)).

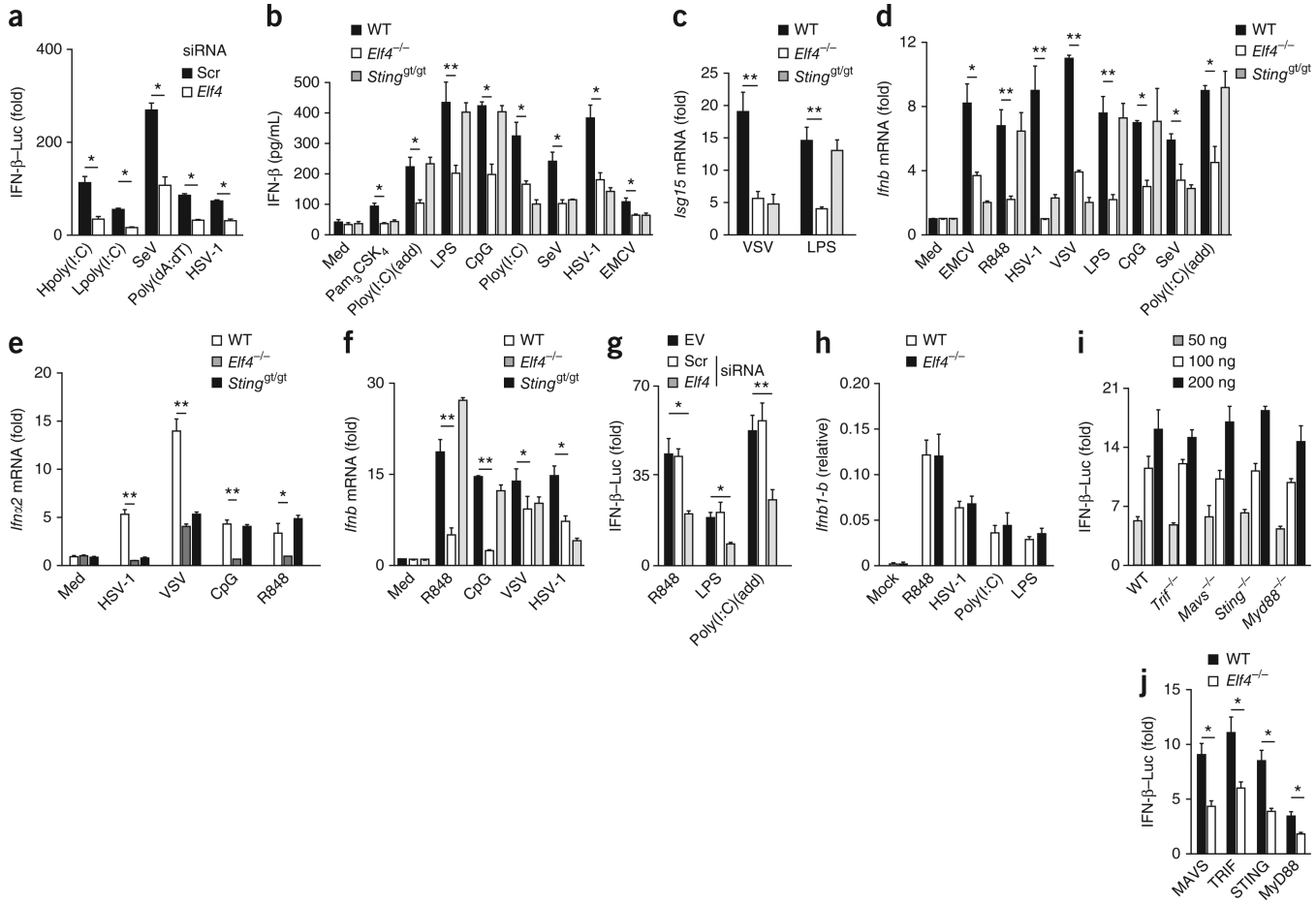

Figure 4.

ELF4 is involved in both the TLR and RLR signaling pathways. (**a**) Luciferase activity of IFN-β in 293T cells expressing IFN-β–Luc plasmid and either scrambled (Scr) or *Elf4*-specific siRNA, after 24 h infection with SeV or HSV-1, or transfection with high-molecular-weight poly(I:C) (Hpoly(I:C)), low-molecular-weight poly(I:C) (Lpoly(I:C)) or poly(dA:dT). (**b,c**) Enzyme-linked immunosorbent assay of IFN-β and qRT-PCR analysis of *Isg15* mRNA, normalized to β-actin expression, in wild-type, *Sting*$^{gt/gt}$ or *Elf4*$^{-/-}$ BMDMs treated with viruses or PRR ligands Pam_3CSK_4, LPS, CpG DNA, poly(I:C) (added to medium; 'add'), or transfected with poly(I:C). (d,e) qRT-PCR analysis of *Ifnb1* and *Ifna2* mRNA, normalized to β-actin expression, in wild-type, *Sting*$^{gt/gt}$ or *Elf4*$^{-/-}$ peritoneal macrophages after 24 h of infection with viruses or treatment with ligands. (**f**) qRT-PCR analysis of *Ifnb1* mRNA, normalized to β-actin expression, in wild-type, *Sting*$^{gt/gt}$ or *Elf4*$^{-/-}$ BMDC after 24 h of infection with viruses or treatment with ligands. (**g**) Luciferase activity of IFN-β in 293-TLR3 cells (treated with ploy(I:C)), 293-TLR4 cells (treated with LPS) and 293-TLR7 cells (treated with R848) expressing scrambled or *Elf4* siRNA and IFN-β–Luc, 6 h after treatment with ligands. (**h**) qRT-PCR analysis of *Il1b1* mRNA, normalized to β-actin expression, in wild-type or *Elf4*$^{-/-}$ peritoneal macrophages 24 h after infection with HSV-1 or treatment with ligands. (**i**) Luciferase activity of IFN-β in wild-type, *Mavs*$^{-/-}$, *Sting*$^{gt/gt}$, *Myd8*$^{-/-}$ or *Trif*$^{-/-}$ MEFs transfected with IFN-β–Luc and indicated amounts of plasmid encoding ELF4. (**j**) Luciferase activity of IFN-β in wild-type or *Elf4*$^{-/-}$ MEFs transfected with MAVS, MyD88, TRIF or STING with IFN-β–Luc plasmids. **P* < 0.05 and ***P* < 0.01

(Student's *t*-test). Data were pooled from two (**i–j**) or three (**a–h**) independent experiments. Error bars, s.e.m. (*n* = 3 cultures).

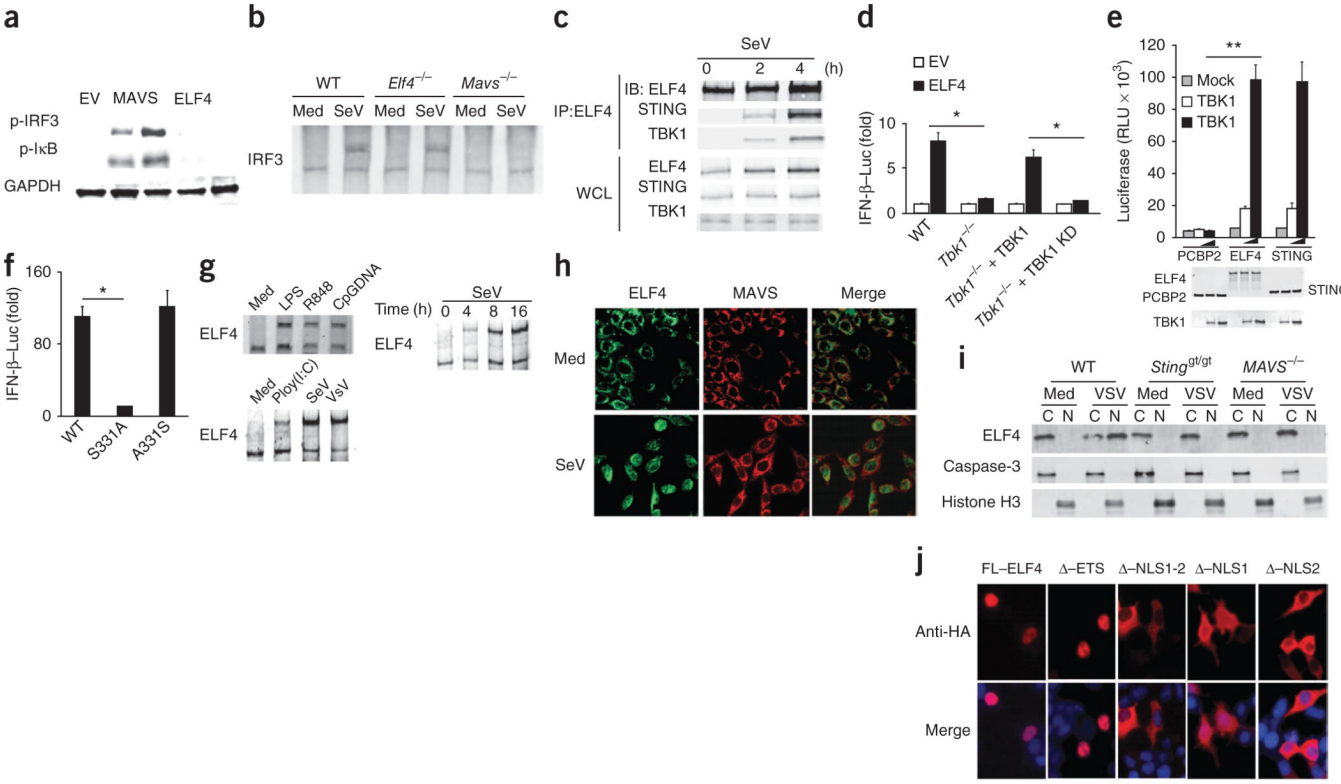

Figure 5.

ELF4 is activated after virus infection but is not required for IRF activation. (**a**) Immunoblot of phosphorylated IRF3 (p-IRF3), phosphorylated IκB (p-IκB) and GAPDH in 293T cells transfected with the empty vector (EV), or 50 ng or 100 ng vector encoding ELF4 or MAVS. (**b**) Native PAGE and immunoblotting showing the dimerization of IRF3 in wild-type, *Mavs*$^{-/-}$ or *Elf4*$^{-/-}$ MEF cells 16 h after infection with SeV or with medium (Med). (**c**) Coimmunoprecipitation and immunoblotting showing the protein interactions in wild-type MEFs infected with SeV. (**d**) Luciferase assay showing the induction of IFN-β in *Tbk1*$^{-/-}$ and wild-type MEFs transfected with plasmids encoding wild-type TBK1 or variants lacking kinase activity, and untransfected cells were transfected with IFN-β–Luc and EV or ELF4. (**e**) Kinase activity of TBK1 using *in vitro*–expressed PCBP2, STING or ELF4 incubated with TBK1, detected by luciferase assay. RLU, relative luciferase units. (**f**) Luciferase activity of IFN-β in 293T cells after 24-h transfection with plasmids encoding wild-type or mutant ELF4. (**g**) Native PAGE and immunoblotting showing the dimerization of ELF4 in peritoneal macrophages or 2fTGH cells treated with ligands or viruses for 6 h or indicated time. (**h**) Confocal microscopy analysis of ELF4 and MAVS in HeLa cells infected with SeV or in medium. Magnification, 25×. (**i**) Immunoblot of ELF4, caspase-3 and histone H3 in cytosol (C) or nucleus (N) of wild-type, *Mavs*$^{-/-}$ or *Sting*$^{gt/gt}$ MEFs 12 h after infection with VSV. (**j**) Immunofluorescence images of HeLa showing the cellular location of full-length ELF4 (FL-ELF4) or the indicated variants of ELF4 in HeLa cells after 24 h transfection with plasmids. Δ-ETS is ELF4 without ETS DNA-binding domain; Δ-NLS1 is ELF4 without the first nuclear localization sequence (NLS); Δ-NLS2 is ELF4 without the second NLS; and Δ-NLS1-2 is ELF4 without both NLSs. Magnification, 25×. **P* < 0.01 and ***P* < 0.001 (Student's *t*-test). Data were pooled from two (**a–c,g–j**) or three (**d–f**) independent experiments. Error bars, s.e.m. (*n* = 3 cultures; **d–f**).

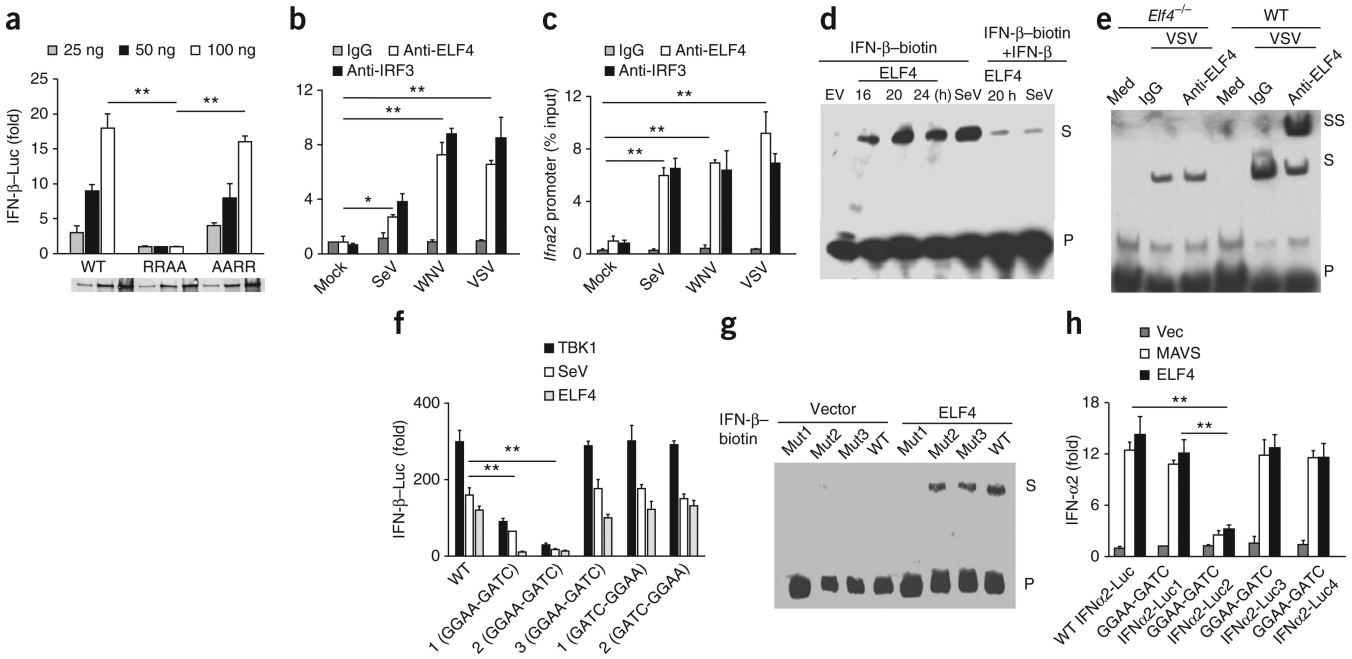

Figure 6.

ELF4 binds to type I interferon promoters. (**a**) Luciferase activity of IFN-β in primary wild-type MEFs transfected with plasmid encoding wild-type or the indicated variant of ELF4. RRAA indicates two arginines replaced by alanines. AARR is 'reversed' substitution. (**b,c**) ChIP assay and qRT-PCR of *Ifnb1* (**b**) and *Ifna2* (**c**) promoter DNA in primary monocyte–derived macrophages 6 h after infection with SeV. Cell lysates were immunoprecipitated by mouse IgG, anti-ELF4 and anti-IRF3. (**d**) EMSA showing the interaction between ELF4 and *Ifnb1* promoter in 293T cells transfected with ELF4 or infected with SeV at the indicated time. Biotinylated probes were detected with HRP-streptavidin. EV, empty vector. (**e**) EMSA of biotinylated *Ifnb1* promoter probes the nuclear extracts in wild-type or *Elf4*$^{-/-}$ MEFs 6 h after infection with VSV. Biotinylated probes were detected with HRP-streptavidin. (**f**) Luciferase activity of IFN-β in 293T cells transfected with plasmids encoding wild-type or the indicated mutant IFN-β–Luc and TBK1 or ELF4, or infected with SeV. (**g**) EMSA showing the interaction between ELF4 and *Ifnb1* promoter. *In vitro*–expressed ELF4 or empty vector (EV) was incubated with the biotinylated wild-type (WT) or GGAA (GGAA to GATC) mutant (mut) *Ifnb1* promoter probes. Biotinylated probes were detected by HRP-streptavidin. (h) Luciferase activity of IFN-α2 in 293T cells co-transfected with indicated amounts of plasmid encoding MAVS or ELF4 and wild-type or mutant IFN-α2–Luc. S marks shifted bands, SS marks supershifted bands, and P marks free probes (**d,e,g**). *$P < 0.05$ and **$P < 0.01$ (Student's *t*-test). Data were pooled from two (**d–e,g**) or three (**a–c,f,j**) independent experiments. Error bars, s.e.m. ($n = 3$ cultures).

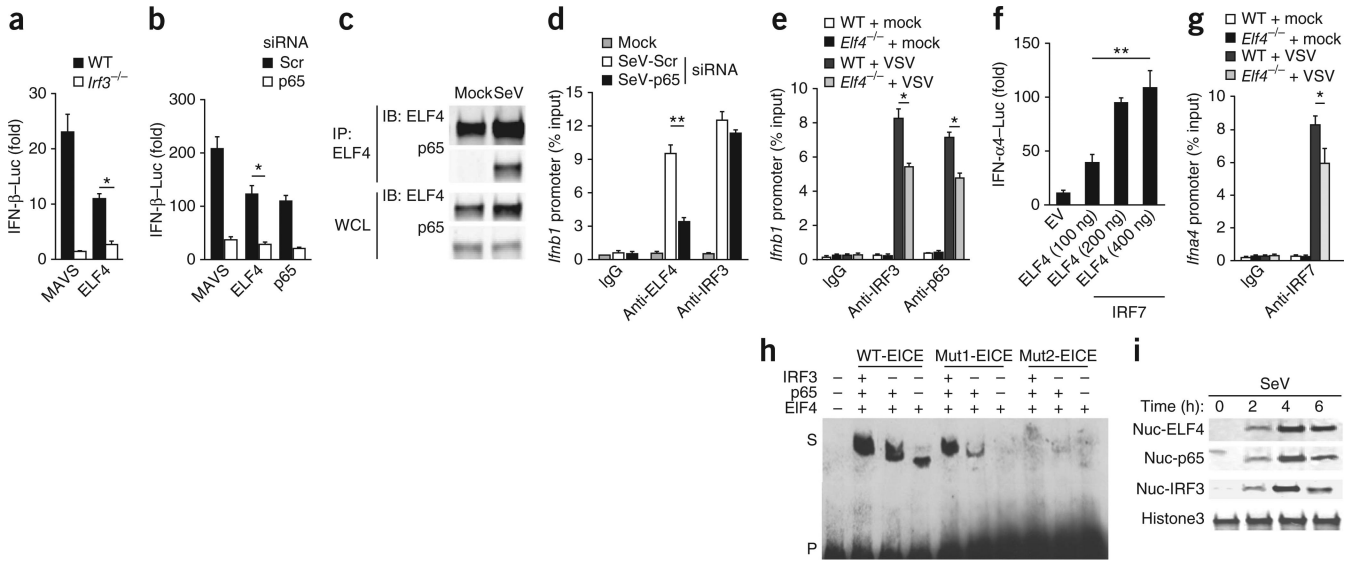

Figure 7.

ELF4 synergizes IRF3, IRF7 and NF-κB to activate interferon production. (**a**) Luciferase activity of IFN-β in wild-type (WT) or *Irf3*$^{-/-}$ MEFs transfected with MAVS or ELF4. (**b**) Luciferase activity of IFN-β in in 293T cells transfected with *Rela* (p65) siRNA or scrambled (Scr) siRNA and MAVS, ELF4 or p65. (**c**) Co-immunoprecipitation and immunoblotting showing the protein interactions in 2fTGH cells infected with SeV for 6 h. (**d**) ChIP assay and qRT-PCR of *Ifnb1* promoter DNA in MEFs expressing scrambled or p65 specific siRNA 6 h after infection with SeV. Cell lysates were immunoprecipitated by mouse IgG, anti-ELF4 or anti-IRF3. (**e,g**) ChIP assay and qRT-PCR of *Ifnb1* (**e**) and *Ifna4* (**g**) promoter DNA in wild-type or *Elf4*$^{-/-}$ peritoneal macrophages infected with VSV for 6 h. Cell lysates were immunoprecipitated by indicated antibodies. (**f**) Luciferase activity of IFN-α4 in wild-type MEFs cotransfected with plasmid encoding IRF7 and empty vector (EV) or indicated amounts of plasmid encoding ELF4. (**h**) EMSA of biotinylated *Ifnb1* promoter probes with WT-EICE (GGAA-GAAA), Mut1-EICE (GATC-GAAA) and Mut2-EICE (GATC-CGGG) and nuclear extracts of 293T cells expressing IRF3, p65 or ELF4, 6 h after infection with SeV. Biotinylated probes were detected by HRP-streptavidin. (i) Immunoblot of IRF3, p65 and ELF4 in nuclear extracts of MEFs infected with SeV at the indicated time. **P* < 0.05 and ***P* < 0.01 (Student's *t*-test). Data were pooled from two (**c,h,i**) or three (**a,b,d–g**) independent experiments. Error bars, s.e.m. (*n* = 3 cultures).